

Single β -AgVO₃ Nanowire H₂S Sensor

Liqiang Mai,^{*,†,‡} Lin Xu,[†] Qian Gao,[†] Chunhua Han,[†] Bin Hu,[†] and Yuqiang Pi[†]

[†]State Key Laboratory of Advanced Technology for Materials Synthesis and Processing, School of Materials Science and Engineering, Wuhan University of Technology, Wuhan, 430070, China, and [‡]Department of Chemistry and Chemical Biology, Harvard University, Cambridge, Massachusetts 02138

ABSTRACT We report the electrical transport and H₂S sensing properties of single β -AgVO₃ nanowire device. β -AgVO₃ nanowires were successfully prepared by ultrasonic treatment followed by hydrothermal reaction using V₂O₅ sol. The individual β -AgVO₃ nanowire exhibits a “threshold switching” phenomenon. High bias (i.e., 6 V for Au contacts) is required to initially switch the individual nanowire device from nonconductive to conductive, and it may be related to the formation of nanoscale metallic Ag when enough voltage is applied between the two electrodes. This novel nanomaterial shows good H₂S sensing performances with short response and recovery time within 20 s, relatively low response concentration of 50 ppm, and good selectivity.

KEYWORDS β -AgVO₃ nanowire, electrical transport, threshold switching, H₂S sensing

In recent years, great attention has been focused on synthesis and applications of one dimensional nanostructured materials such as nanowires, nanobelts, nanorods, and nanotubes.^{1–7} Because of their unique structures and different excellent properties from bulk materials, they have wide-ranging potential applications in areas such as field effect transistors, ultrasensitive nanosize gas sensors, nanoresonators, nanocantilevers, nanogenerators and solar cells.^{8–15}

Vanadium oxide related compounds have unique physical and chemical properties, and they have wide applications such as electrochromic devices, cathodic electrodes for lithium batteries, catalysts, gas sensors, and electrical and optical devices. Among them, silver vanadium oxide (SVO) is a very important kind of chemical compound with good electrochemical property demonstrated by many researchers.^{16,17} β -AgVO₃ is a stable phase and a typical silver vanadium oxide.¹⁸ Its properties highly depend on the synthesis method, size, morphology, crystal structure and surface properties of the product.^{19,20} Over the past years, there have been some reports on the synthesis of β -AgVO₃ nanomaterials, and their electrical, electrochemical, photochemical, and electrochromic properties have been discussed. Until now, however, there is little understanding of gas sensing properties of β -AgVO₃, which limits the wide application of this kind of novel nanomaterials.

As we know, H₂S is a malodorous toxic gas. It can lead to personal distress at low concentrations, and may cause death when the concentration is higher than 250 ppm,²¹ so it is of great interest to develop a reliable and effective H₂S gas sensor. Several groups have been focusing on H₂S detection. Muben et al.²² reported novel gas nanosensors consisting of gold nanoparticles electrodeposited on SWNTs

that could sense H₂S in air at room temperature with a 3 ppb limit of detection. The response time was typically in the range of 6–8 min for all selected concentrations, while the recovery time was even longer. Shirsat et al.²³ reported on the synthesis and H₂S gas sensing performance of the networks made of hybrid polyaniline (PANI) nanowires and gold nanoparticles at room temperature. The sensor showed a linear response to H₂S from 0.1 to 500 ppb in air, and had a response time within 2 min and a recovery time within 5 min. Chen et al.²⁴ demonstrated H₂S detection of 500 ppb to 1000 ppm at 160 °C using vertically aligned CuO nanowire array sensors. However, when the concentration went to higher than 5 ppm, the response became unrecoverable. Rout et al.²⁵ reported H₂S sensors based on tungsten oxide nanostructures over the 1–1000 ppm concentration range at 40–250 °C and found that the nanoparticles and nanoplatelets of WO₃ exhibited high response values. The response times varied in the 55–100 s range for the nanoplatelets, whereas for the nanoparticles the response time was 80–130 s. The recovery times of all the nanostructures were in the 18–40 s range depending on the temperature. Tao et al.²⁶ discussed the H₂S sensing properties of noble metal doped WO₃ thin film sensor fabricated by micromachining. These sensors were promising for H₂S gas detection in the range from 1 to 100 ppm; the response times of Pt-, Au–Pt-, and Au-doped WO₃ thin films were 30, 2, and 8 s, and the recovery times were about 30, 30, and 160 s, respectively. Liao et al.²⁷ prepared ZnO nanorod gas sensors for H₂S detection and found that the thin nanorods had a significantly better sensing performance than the thick nanorods. But the response and recovery times to H₂S were long at room temperature. Kong et al.²⁸ showed that the sensitivity of CuO–SnO₂ nanoribbon sensor was as high as 18 000. The response time was 15 s at room temperature and increased with temperature. When the temperature was about 175 °C, the response time was about 5 min. On the other hand, the recovery time on removal of H₂S was slow

* To whom correspondence should be addressed. E-mail: mlq@cmliris.harvard.edu.

Received for review: 04/15/2010

Published on Web: 05/26/2010



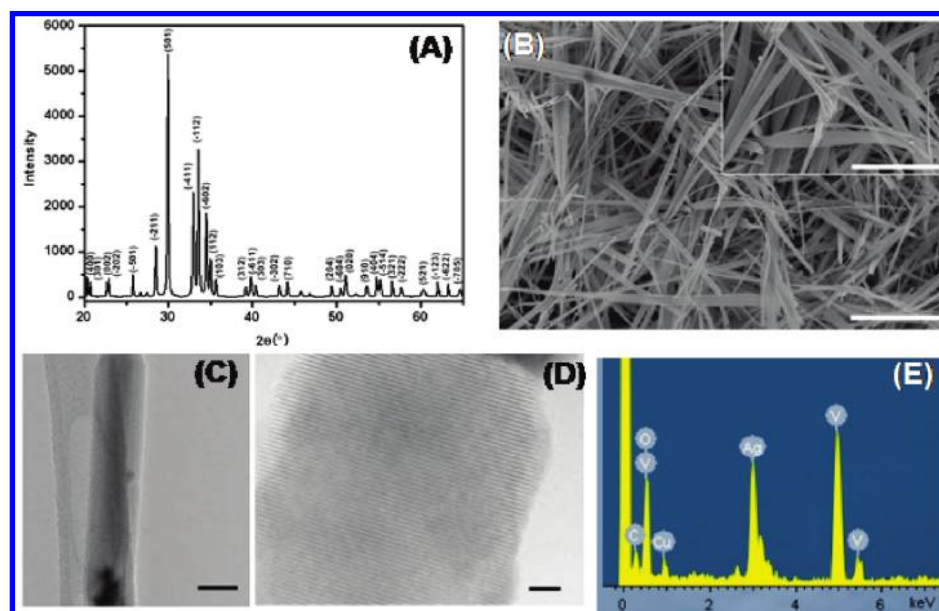


FIGURE 1. XRD pattern (A), SEM (B) (scale bar is 10 μm , the inset in (B) is high-magnification SEM image (scale bar is 5 μm)), TEM (C) (scale bar is 40 nm), HRTEM (D) (scale bar is 2 nm) images, and EDS spectra (E) of the obtained $\beta\text{-AgVO}_3$.

(about several tens of minutes at room temperature) but improved with temperature. Sun et al.²⁹ reported a catalytic chemiluminescence sensor made of $\alpha\text{-Fe}_2\text{O}_3$ nanotubes for rapid and selective detection of H_2S down to 10 ppm at 110 $^\circ\text{C}$ with a short response time of 15 s and a recovery time of less than 100 s. In the present work, we report the electrical transport and H_2S sensing properties of single $\beta\text{-AgVO}_3$ nanowire devices.

$\beta\text{-AgVO}_3$ nanowires were successfully prepared by ultrasonic treatment followed by hydrothermal reaction using V_2O_5 sol.^{4,30} Briefly, the as-prepared V_2O_5 sol and Ag_2O powder were mixed by stirring and ultrasonic treatment, then transferred into a Teflon-lined stainless steel autoclave and kept at 180 $^\circ\text{C}$ for 1 d. The products were collected and washed repeatedly with distilled water and finally dried at 80 $^\circ\text{C}$ in air for 12 h.

To determine the phase structures of the products, the X-Ray Diffraction (XRD) measurements were conducted. The XRD pattern of the as-synthesized product is shown in Figure 1A. It can be assigned to the phase of $\beta\text{-AgVO}_3$ monoclinic structure [space group $I2/m(12)$],³¹ which is in good agreement with JCPDS card 29-1154. No obvious peaks of other phases are detected, indicating that the product is composed mainly of $\beta\text{-AgVO}_3$.

Figure 1B shows scanning electron microscopy (SEM) images of the obtained $\beta\text{-AgVO}_3$, which reveal that the resulting product is composed mainly of flexible nanowires with well-defined facets. The width and thickness of the nanowires are in the range of 100–700 and 50–100 nm, respectively, with typical lengths up to several tens of micrometers.

The wire-like $\beta\text{-AgVO}_3$ is further characterized and confirmed by transmission electron microscopy (TEM) tech-

nique (Figure 1C). The high-resolution transmission electron microscopy (HRTEM) image (Figure 1D) taken from the nanowire shows lattice spacing of 0.3522 nm corresponding to the lattice spacing of the (110) plane of $\beta\text{-AgVO}_3$, which indicates the possible preferential plane of the $\beta\text{-AgVO}_3$ nanowire. Energy dispersive spectroscopy (EDS) investigation taken from the nanowire (Figure 1E) indicates the presence of Ag, V, and O elements, which agrees well with the result of XRD analysis.

To measure the electrical transport along a single nanowire, a single nanowire was placed across two gold electrodes, and the final contacts were improved by Pt deposition at the two ends.^{32,33} The single nanowire exhibits a “threshold switching” phenomenon. Notably, high bias (>6 V) is required to initially switch the individual nanowire device from nonconductive to conductive (Figure 2A). Figure 2B shows the typical I – V curves of the single nanowire at room temperature (25 $^\circ\text{C}$) and 250 $^\circ\text{C}$ after applying high bias of 6 V, showing a typical semiconductor behavior. The current level is 3–6 μA at the bias of 1 V, 2–3 orders magnitude higher than those reported by others.^{17,20} Device fabricated with Al metal contacts also exhibits similar “threshold switching” phenomenon, while the threshold voltage decreases to 1 V.

Electrical switching is usually to be realized by phase transformation such as Mott metal–insulator transition (MIT) when a voltage is applied between the two electrodes.³⁴ But threshold switching has also appeared in many chalcogenide glass systems lacking phase behavior. In this case, a highly conductive transitory filament is usually conceived, which may be electronic in nature. The latter explanation might be applicable here and electrical switching of $\beta\text{-AgVO}_3$ nanowire may be related to the formation of nanoscale

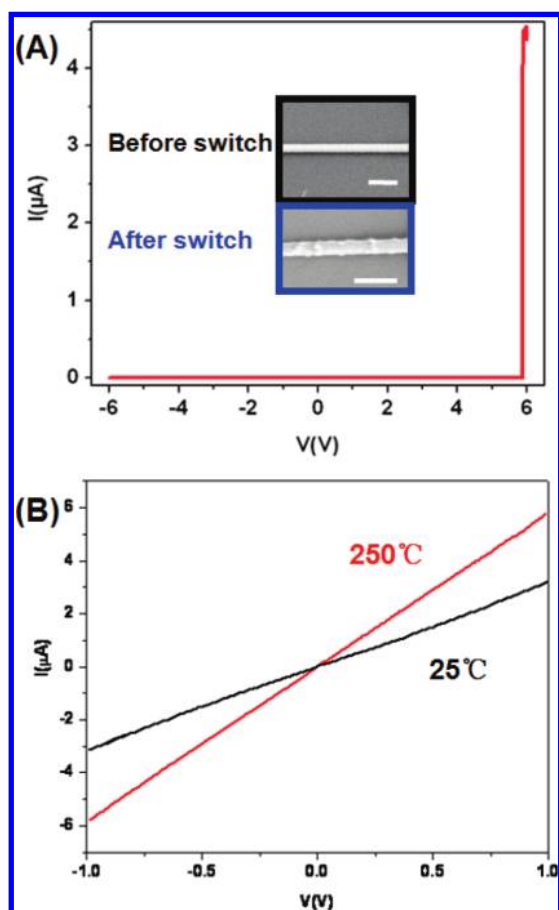


FIGURE 2. I/V curves of individual β - AgVO_3 nanowire at high bias of 6 V (A) and at the bias of 1 V after applying high bias of 6 V at 25 and 250 °C (B) (the inset in (A) shows the corresponding SEM image of the individual β - AgVO_3 nanowire before and after switch, scale bar is 600 nm).

metallic Ag when enough voltage is applied between the two electrodes.³⁵

Applying voltage may result in resistively heating, which plays the similar role with high-energy electron beam irradiation heating.^{34,36–39} To investigate the possible relation between electrical switching of β - AgVO_3 NW and the formation of nanoscale Ag, we conducted high-energy electron beam irradiation heating experiment during TEM observation. Interestingly, many nanoparticles with the diameter of several nanometers to 20 nm are in situ formed under bombardment (~ 10 s) of high-energy electrons during TEM observation, which is shown in Figure 3A. HRTEM image (Figure 3B) taken from the typical nanoparticle shows lattice spacing of 0.2370 nm, coinciding with the lattice spacing of the (111) plane of cubic Ag phase. Very strong intensity of Ag peak in the EDS spectrum taken from the typical nanoparticle (Figure 3C) also indicates in situ formation of Ag nanoparticles, which may correspond with the rough surface of the nanowire after switch (inset of Figure 2A).

To study the H_2S sensing performance, an individual β - AgVO_3 nanowire device was placed in a vacuum chamber having a special gas injector to accurately control the quan-

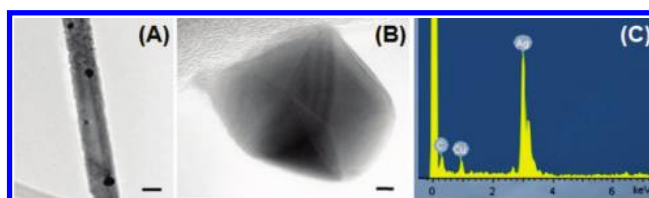


FIGURE 3. TEM image of a single nanowire (A) (scale bar is 40 nm), HRTEM image of the nanoparticle on the surface of the nanowire (B) (scale bar is 2 nm) and EDS spectra (C) after high-energy electrons exposure using TEM for ~ 10 s.

tity of injecting gas.³² Figure 4A shows the typical response curve of resistance with time on switching the gases from Ar to different concentration at 250 °C. Upon exposure to H_2S , the resistance decreases quickly and then gets saturated, while on cutting off the H_2S supply the resistance increases and returns nearly to its baseline value. After several circles between the test gas and Argon, the nanowire sensor can still recover to the initial states, indicating good reversibility.

The plot in Figure 4B shows the sensitivities of the sensor to H_2S with different concentrations. According to literature, there are usually two different definitions of gas sensitivity. One is defined as $(R_a - R_g)/R_a$ in most cases,⁴⁰ and the other is defined as R_a/R_g for the reducing gas,⁴¹ where R_g and R_a are the electrical resistances of the sensor in the measuring gas and in clean air, respectively. In our case, considering that the resistance of the sensor in Ar (R_{Ar}) is high and resistance changes in the test gas (R_g) are relatively small, we define the gas sensitivity as the ratio of resistance of the sensor in Ar (R_{Ar}) and in the test gas (R_g) as follows

$$\text{Sensitivity} = \frac{R_{Ar}}{R_g} \quad (1)$$

Notably, the nanowire exhibits an impressive sensing response toward H_2S even at the relatively low concentration of 50 ppm. The sensitivity increases with the increase of the gas concentration between 50 and 400 ppm. Our preliminary results also show that low detection limits may be improved by surface modification and structure and crystalline optimization and by other treatments of β - AgVO_3 nanowires. Further research work is under way. It is also observed that the sensitivity increases with the increase of the gas concentration between 50 and 400 ppm.

Figure 4C shows the response/recovery time with different concentrations, which is defined as the time required to reach 90% of the final equilibrium value. The response time and recovery time are both within 20 s, and the recovery time is relatively short (< 10 s). The shortest response time is only 4 s, when the gas concentration is 300 ppm. And the recovery time is longer than the response time, which is in accordance with the results of most references.^{25,26,28,29}

Recently, efforts have been endeavored to improve H_2S sensing properties such as low detection limit, wide dynamic

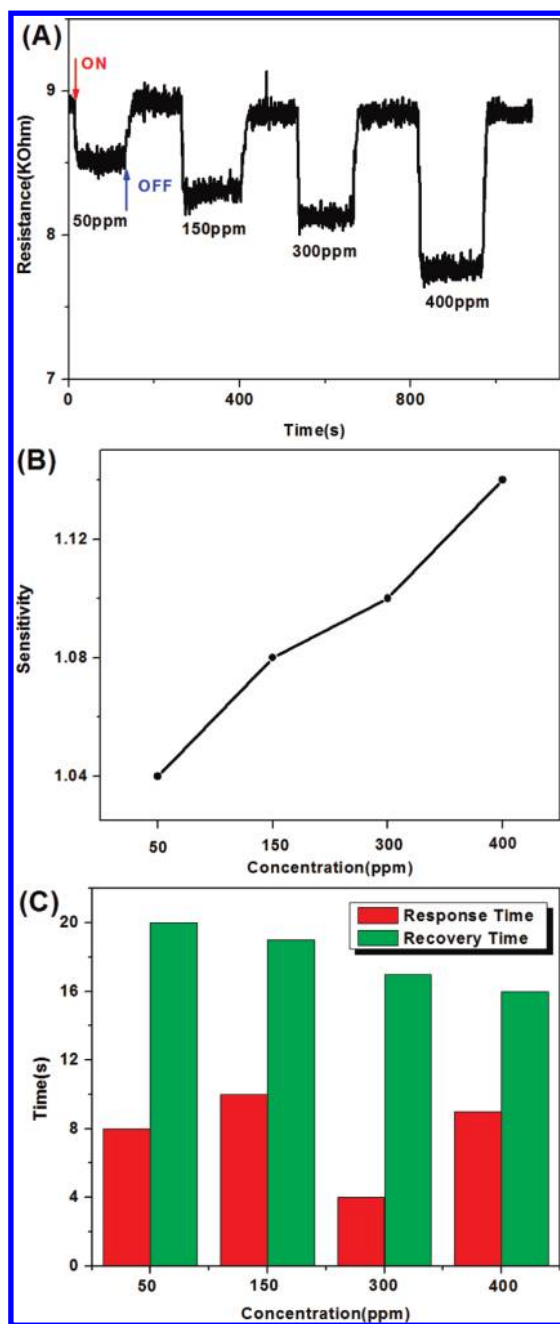


FIGURE 4. (A) The response curve of resistance with time on switching the gases from Ar to different concentrations at 250 °C. (B) the sensitivities of the nanowire toward H₂S at a working temperature of 250 °C. (C) The response/recovery time with different concentrations.

range, high response, low-operating temperature, short response and recovery time, reproducibility, and selectivity. According to literature, many kinds of materials have been chosen for H₂S detecting. The detection limit of H₂S is low to ppb scale and the response is high. Some H₂S sensors can be operated at room temperature. However, they cannot meet all the aspects of advantages and most of their response and recovery time are long to minute scale. To the best of our knowledge, there are no reports about H₂S

sensing property of β -AgVO₃ bulk materials. Our results show that the β -AgVO₃ based H₂S sensor performances with short response and recovery time within 20 s from Ar to 50–400 ppm H₂S at 250 °C, which is helpful for the design of new kind of nanodevices.

With regard to practical application, the selectivity of gas sensor is also an important parameter. Therefore, H₂ and CO sensing properties of single β -AgVO₃ nanowire was also measured under the same condition. Notably, in our case, the response to H₂ and CO and the change of response were very slight when the sensor exposed in different concentrations of H₂ and CO, respectively, which indicates that the sensor has good selectivity to H₂S.

The mechanism of sensing by β -AgVO₃ is probably explained by the modulation model of the depletion layer,⁴² which is surface controlled; in this mechanism, the grain size, surface states, and oxygen adsorption play important roles.^{43–45} In our case, although the sensor performances of single β -AgVO₃ nanowire devices were related to several factors, such as the gap between electrodes, electrode width, and metal surface modification, it was undeniable that Ag nanoparticles formed on the surface of single β -AgVO₃ nanowires during sensing were probably helpful to the gas sensing process. The exact mechanism is still being investigated.

In conclusion, β -AgVO₃ nanowires were synthesized using hydrothermal reaction with ultrasonic treatment from V₂O₅ sol as the reactant. Electrical transport measurements show “threshold switching” characteristic of the single nanowire, and the threshold voltage is 6 V with Au contacts. After applying high bias of 6 V to switch the individual nanowire from nonconductive to conductive, it exhibits linear, symmetric current/voltage (*I/V*) characteristics with a current level 2–3 orders magnitude higher than that reported by others. Single β -AgVO₃ nanowire shows good gas sensing property to H₂S. This novel nanomaterial exhibits short response and recovery time within 20 s, relatively low response concentration of 50 ppm, and good selectivity, which offers possible and potential applications as a H₂S sensor.

Acknowledgment. This work was supported by the National Nature Science Foundation of China (50702039), the Research Fund for the Doctoral Program of Higher Education (20070497012), the Scientific Research Foundation for Returned Scholars, the Ministry of Education of China (2008-890), and the Innovation Special Foundation of Excellent Returned Scholars of Wuhan (2008-84). Thanks to Prof. C. M. Lieber and Dr. Y. J. Dong of Harvard University, Prof. Z. L. Wang, Dr. Q. Kuang, and Dr. J. Zhou of Georgia Institute of Technology, Prof. W. Chen, Mr. B. Hu, and Dr. W. Jin of Wuhan University of Technology for strong support and stimulating discussion. We want to thank Dr. Y. Z. Huang of University of Oxford, and Prof. C. W. Zhao of Inner Mongolia University of Technology for their help and collaboration in TEM analysis and structure characterization.

REFERENCES AND NOTES

- (1) Dai, H. J.; Wong, E. W.; Lu, Y. Z.; Fan, S. S.; Lieber, C. M. *Nature* **1995**, *375*, 769–772.
- (2) Morales, A. M.; Lieber, C. M. *Science* **1998**, *279*, 208–211.
- (3) Cui, Y.; Wei, Q. Q.; Park, H. K.; Lieber, C. M. *Science* **2001**, *293*, 1289–1292.
- (4) Mai, L. Q.; Hu, B.; Hu, T.; Chen, W.; Gu, E. D. *J. Phys. Chem. B* **2006**, *110*, 19083–19086.
- (5) Mai, L. Q.; Hu, B.; Chen, W.; Qi, Y. Y.; Lao, C. S.; Yang, R. S.; Dai, Y.; Zhong, L. W. *Adv. Mater.* **2007**, *19*, 3712–3716.
- (6) Mai, L. Q.; Guo, W. L.; Hu, B. *J. Phys. Chem. C* **2008**, *112*, 423–429.
- (7) Mai, L. Q.; Gu, Y. H.; Han, C. H.; Hu, B.; Chen, W.; Zhang, P. C.; Xu, L.; Guo, W. L.; Dai, Y. *Nano Lett.* **2009**, *9*, 826–830.
- (8) Tian, B. Z.; Zheng, X. L.; Kempa, T. J.; Fang, Y.; Yu, N. F.; Yu, G. H.; Huang, J. L.; Lieber, C. M. *Nature* **2007**, *449*, 885–889.
- (9) Mao, C. J.; Wu, X. C.; Pan, H. C.; Chen, H. Y. *Nanotechnology* **2005**, *16*, 2892–2896.
- (10) Lu, W.; Lieber, C. M. *Nat. Mater.* **2007**, *6*, 841–850.
- (11) Mai, L. Q.; Lao, C. S.; Hu, B.; Zhou, J.; Qi, Y. Y.; Chen, W.; Gu, E. D.; Zhong, Z. L. *J. Phys. Chem. B* **2006**, *110*, 18138–18141.
- (12) Wang, J. F.; Gudiksen, M. S.; Duan, X. F.; Cui, Y.; Lieber, C. M. *Science* **2001**, *293*, 1455–1457.
- (13) Patolsky, F.; Timko, B. P.; Yu, G. H.; Fang, Y.; Greytak, A. B.; Zheng, G. F.; Lieber, C. M. *Science* **2006**, *313*, 1100–1104.
- (14) Whang, D.; Jin, S.; Wu, Y.; Lieber, C. M. *Nano Lett.* **2003**, *3*, 1255–1259.
- (15) Wang, Z. L.; Song, J. H. *Science* **2006**, *312*, 242–246.
- (16) Zhang, S. Y.; Li, W. Y.; Li, C. S.; Chen, J. J. *J. Phys. Chem. B* **2006**, *110*, 24855–24863.
- (17) Song, J. M.; Lin, Y. Z.; Yao, H. B.; Fan, F. J.; Li, X. G.; Yu, S. H. *ACS Nano* **2009**, *3*, 653–660.
- (18) Liu, S. W.; Wang, W. Z.; Zhou, L.; Zhang, L. S. *J. Cryst. Growth* **2006**, *293*, 404–408.
- (19) Xie, J. G.; Cao, X. Y.; Li, J. X.; Zhan, H.; Xia, Y. Y. *Ultrason. Sonochem.* **2005**, *12*, 289–293.
- (20) Bao, S. J.; Bao, Q. L.; Li, C. M.; Chen, T. P.; Sun, C. Q.; Dong, Z. L.; Gan, Y.; Zhang, J. *Small* **2007**, *3*, 1–4.
- (21) Tao, W. H.; Tsai, C. H. *Sens. Actuators, B* **2002**, *81*, 237–247.
- (22) Muben, S.; Zhang, T.; Chartuprayoon, N.; Rheem, Y.; Mulchandani, A.; Myung, A. V.; Deshusses, M. A. *Anal. Chem.* **2010**, *82*, 250–257.
- (23) Shirsat, M. D.; Bangar, M. A.; Deshusses, M. A.; Myung, N. V.; Mulchandani, A. *Appl. Phys. Lett.* **2009**, *94*, No. 083502.
- (24) Chen, J.; Wang, K.; Hartman, L.; Zhou, W. *J. Phys. Chem. C* **2008**, *112*, 16017–16021.
- (25) Rout, C. S.; Hegde, M.; Rao, C. N. R. *Sens. Actuators, B* **2008**, *128*, 488–493.
- (26) Tao, W. H.; Tsai, C. H. *Sens. Actuators, B* **2002**, *81*, 237–247.
- (27) Liao, L.; Lu, H. B.; Li, J. C.; He, H.; Wang, D. F.; Fu, D. J.; Liu, C. *J. Phys. Chem. C* **2007**, *111*, 1900–1903.
- (28) Kong, X. H.; Li, Y. D. *Sens. Actuators, B* **2005**, *105*, 449–453.
- (29) Sun, Z. Y.; Yuan, H. Q.; Liu, Z. M.; Han, B. X.; Zhang, X. R. *Adv. Mater.* **2005**, *17*, 2993–2997.
- (30) β -AgVO₃ nanowires were synthesized as follows: V₂O₅ powder was molten at 800 °C in a ceramic crucible. When the molten liquid was quickly poured into distilled water, a brownish V₂O₅ sol was formed. Then, the as-prepared V₂O₅ sol and Ag₂O were mixed together in the molar ratio of 1:1. After stirring and ultrasonic treatment, the solution was transferred into a Teflon-lined stainless steel autoclave and kept at 180 °C for 1 day. Then the autoclave was left to cool down in air, and the orange precipitate was obtained. The products were collected and washed repeatedly with distilled water, and finally dried at 80 °C in air for 12h.
- (31) Taraci, J. L.; Hÿtch, M. J.; Clement, T.; Peralta, P.; McCartney, M. R.; Drucker, J.; Picraux, S. T. *Nanotechnology* **2005**, *16*, 2365–2371.
- (32) Kuang, Q.; Lao, C. S.; Li, Z.; Liu, Y. Z.; Xie, Z. X.; Zheng, L. S.; Wang, Z. L. *J. Phys. Chem. C* **2008**, *112*, 11539–11544.
- (33) The as-synthesized β -AgVO₃ nanowires were collected and dispersed in ethanol, then transferred onto a silicon substrate with predefined Au electrodes; so the nanowire was lying across the Au electrodes. These devices were further fabricated using focused ion beam (FIB) deposition to deposit a 500 nm thick Pt layer on the contact point of the β -AgVO₃ nanowire and the Au electrode to improve the contacts.
- (34) Baik, J. M.; Kim, M. H.; Larson, C.; Yavuz, C. T.; Stucky, G. D.; Wodtke, A. M.; Moskovits, M. *Nano Lett.* **2009**, *9*, 3980–3984.
- (35) Schoen, D. T.; Xie, C.; Cui, Y. *J. Am. Chem. Soc.* **2007**, *129*, 4116–4117.
- (36) Zhang, H. F.; Wang, C. M.; Buck, E. C.; Wang, L. S. *Nano Lett.* **2003**, *3*, 557–580.
- (37) Molchan, I. S.; Thompson, G. E.; Skeldon, P.; Andriessen, R. J. *Colloid Interface Sci.* **2008**, *323*, 282–285.
- (38) Baik, J. M.; Kim, M. H.; Larson, C.; Wodtke, A. M.; Moskovits, M. *J. Phys. Chem. C* **2008**, *112*, 13328–13331.
- (39) Strelcov, E.; Lilach, Y.; Kolmakov, A. *Nano Lett.* **2009**, *9*, 2322–2326.
- (40) Bhattacharyya, P.; Basu, P. K.; Saha, H.; Basu, S. *Sens. Actuators, B* **2007**, *124*, 62–67.
- (41) Barazzouk, S.; Tandon, R. P.; Hotchandani, S. *Sens. Actuators, B* **2006**, *119*, 691–694.
- (42) Gergintschew, Z.; Förster, H.; Kositzka, J.; Schipanski, D. *Sens. Actuators, B* **1995**, *170*, 26–27.
- (43) Rothschild, A.; Komem, Y. *J. Appl. Phys.* **2004**, *95*, 6374–6380.
- (44) Franke, M. E.; Koplin, T. J.; Simon, U. *Small* **2006**, *2*, 36–50.
- (45) Jin, W.; Dong, B. T.; Chen, W.; Zhao, C. X.; Mai, L. Q.; Dai, Y. *Sens. Actuators, B* **2010**, *145*, 211–215.